IEEE Access
Multidisciplinary | Rapid Review | Open Access Journal

Received October 4, 2016, accepted October 13, 2016, date of publication October 19, 2016, date of current version November 8, 2016.

Digital Object Identifier 10.1109/ACCESS.2016.2618772

Virtual Spatial Modulation

JUN LI[1], MIAOWEN WEN[2], (Member, IEEE), MENG ZHANG[3], AND XIANG CHENG[3], (Senior Member, IEEE)

[1]Department of Electronics and Information Engineering, Chonbuk National University, Jeonju 561-756, South Korea
[2]School of Electronic and Information Engineering, South China University of Technology, Guangzhou 510641, China
[3]State Key Laboratory of Advanced Optical Communication Systems and Networks, School of Electrical Engineering and Computer Science, Peking University, Beijing 100871, China

Corresponding author: M. Wen (eemwwen@scut.edu.cn)

This work was supported by the National Nature Science Foundation of China under Grant 61501190, Grant 61201249, Grant 61622101, and Grant 61571020, and the Nature Science Foundation of Guangdong Province under Grant 2014A030310389.

ABSTRACT In this paper, we propose a virtual spatial modulation (VSM) scheme that performs index modulation on the virtual parallel channels resulting from the singular value decomposition of the multi-input-multi-output channels. The VSM scheme conveys information through both the indices of the virtual parallel channels and the M-ary modulated symbols. We derive a closed-form upper bound on the average bit error probability (ABEP), which considers the impact of imperfect channel estimation. Moreover, the asymptotic ABEP is also studied, which characterizes the error floor under imperfect channel estimation and the resulting diversity order as well as the coding gain under perfect channel estimation. Computer simulations verify the analysis and show that the VSM scheme can outperform the existing pre-coding aided spatial modulation schemes under the same spectral efficiency.

INDEX TERMS Singular value decomposition (SVD), pre-coding, spatial modulation, average bit error probability.

I. INTRODUCTION

Multi-input-multi-output (MIMO) systems can greatly increase the channel capacity without sacrificing additional spectral resources in wireless communications [1], [2]. Various well-known categories of MIMO techniques, such as vertical-bell laboratories layered space-time (V-BLAST) [3] and space time block coding [4], have been proposed to exploit the benefits. However, several problems imply in MIMO systems due to the activation of multiple transmit antennas, such as the requirements of multiple radio frequency (RF) chains and inter-antenna synchronization, and the arising of the inter-channel interference (ICI).

To overcome above-mentioned problems, spatial modulation (SM) [5]–[8] has been proposed recently, in which only a single transmit antenna is activated for each transmission. Since a single RF chain is needed, SM leads to low transceiver complexity and low power consumption, which is beneficial for practical application [9], [10]. Note that the impact of channel estimation on the performance of SM or SSK has also been studied in more practical systems [11], [12]. Following the idea of SM, a great deal of works have been proposed. In [13], space shift keying (SSK), which only relies on the index of the active antenna to convey information, is proposed to mitigate the implementation burden of SM. Generalized SSK (GSSK) [14] and SM (GSM) [15] extend SSK and SM by allowing activation of more than one transmit antenna, which enhance the spectral efficiencies of SSK and SM, respectively. The applications of SM and SSK into the relay systems are provided in [16] and [17]. In [18], quadrature SM (QSM), which expands the spatial domain to include both real and imaginary domains, is also proposed to increase the spectral efficiency of SM. Combining SM with trellis coding and space time block coding (STBC), more extensions, such as trellis coded SM (TCSM) and STBC-SM, have been proposed to improve the transmit diversity of SM [19]–[21]. To dispense with the channel estimation at the receiver, differential SM (DSM) is proposed in [22] and [23], which utilizes the antenna activation order to convey additional information.

More recently, the concept of SM is further extended to the receiver side. In [24], in favor of the zero-forcing (ZF) or minimum mean square error (MMSE) pre-coding, pre-coding SM (PSM) is proposed, which activates a single receive antenna at each time slot and conveys additional information through its index. At the cost of the requirement of channel state information (CSI) at the transmitter, PSM is shown to outperform most transmitter-side SM schemes and the

conventional MIMO scheme. Attracted by its advantages, plenty of works related to PSM have also been proposed [25]–[29]. Generalised PSM (GPSM), which allows PSM to activate multiple receive antennas, is designed in [25]. The extension of GPSM into the multi-stream system is investigated in [26]. In [27], generalised pre-coding aided quadrature SM (GPQSM) is proposed as another extension of PSM, where the transmitted information is further embedded into the real and imaginary signals. By regarding the distributed relays as receive antennas, the idea of PSM is applied in a dual-hop relaying, where the source node of multiple antennas employs pre-coding operation to select a single relay, whose index carries information, to forward signals in an SM manner to the destination node [28]. Following [28] and [29] proposes the use of pre-coding aided DSM instead of PSM for the source node to avoid channel estimation at all receiving nodes.

All above-mentioned pre-coding schemes require the ZF or MMSE pre-coding to transfer the MIMO channel into multiple parallel channels. To apply, however, the number of transmit antennas, N_t, must not be less than that of receive antennas, N_r. On the other hand, the complete elimination of ICI by the ZF or MMSE pre-coding incurs high correlation between the resulting parallel channels. The correlated channels, however, will seriously deteriorate the performance of an index modulation system, which relies on the diversity of channels to convey information. The above observation motivates us to propose a novel pre-coding scheme, named virtual SM (VSM), which transfers the MIMO channels into virtual parallel channels with less channel correlation. The VSM scheme exploits the indices of the virtual parallel channels resulting from the singular value decomposition (SVD) of the MIMO channel to convey information. The right unitary matrix is chosen as the pre-coding matrix. For ease of implementation, a low-complexity near-optimal detector is also designed. Assuming Rayleigh fading channels, we study the average bit error probability (ABEP) of the VSM scheme, which takes into account the impact of imperfect channel estimation. Specifically, according to the union bounding technique, we derive a closed-from upper bound on the ABEP. In addition, inspired by [30] and [31], an asymptotic expression of ABEP in the high signal-to-noise ratio (SNR) region is also provided, which characterizes the ABEP error floor with channel estimation errors and the diversity order as well as coding gain without channel estimation errors. Computer simulations are conducted to investigate the performance of the VSM scheme. Results show that the VSM scheme significantly reduces the ABEP error floor under imperfect channel estimation and achieves the same diversity order of $N_t - N_r + 1$ as the existing receiver-side SM schemes while obtaining a much higher coding gain.

The rest of this paper is organized as follows. In Section II, we introduce the system model and the GPQSM scheme. The principle and the implementation of the VSM scheme are clarified in Section III. Section IV presents the ABEP upper bound and asymptotic analysis for the VSM scheme. In Section V, comparisons in terms of the ABEP are made. Finally, this paper is concluded in Section VI.

Notations: Upper and lower case boldface letters denote matrices and column vectors, respectively. The complex number field is represented by $\mathbb{C}$. $(\cdot)^T$, $(\cdot)^H$ and $(\cdot)^{-1}$ represent the transpose, Hermitian transpose and inversion operations, respectively. $\mathbf{I}_M$ is an identity matrix of size $M \times M$. $\mathrm{Tr}\{\mathbf{X}\}$ returns the trace of the matrix $\mathbf{X}$. $||\cdot||$ and $\mathrm{C}(\cdot,\cdot)$ denote the Frobenius norm and binomial operations, respectively. $Q(\cdot)$ and $\Re\{\cdot\}$ represent the Gaussian Q-function [32] and the real component of the argument, respectively. $\mathrm{diag}\{\mathbf{x}\}$ denotes a diagonal matrix whose diagonal elements are drawn from $\mathbf{x}$. The probability density function (PDF) and the probability of an event are denoted by $f(\cdot)$ and $\Pr(\cdot)$, respectively. $\Gamma(z)$ denotes the Gamma function, which is given by $\Gamma(z) = x^z \int_0^{+\infty} e^{-xt} t^{z-1} dt$ [33]. $\mathrm{sort}(\cdot)$ denotes an ordering function that reorders the elements in an ascending order.

II. SYSTEM MODEL AND OVERVIEW OF GPQSM

A. SYSTEM MODEL

We consider a MIMO system with an M-ary constellation set $\mathcal{S}$, N_t transmit and N_r receive antennas. The MIMO channels are denoted by $\mathbf{H} \in \mathbb{C}^{N_r \times N_t}$, where $h_{i,j}$ with $i \in \{1, \ldots, N_r\}$ and $j \in \{1, \ldots, N_t\}$ denotes the channel between the j-th transmit antenna to the i-th receive antenna, which is assumed to be a complex Gaussian random variable (RV) with zero mean and unit variance. For simplicity, we do not take into account the channel correlation, which implies that the entries of $\mathbf{H}$ are independent of each other. The received signal vector with pre-coding for all schemes can be expressed in a general form as

$$\mathbf{y} = \mathbf{HPx} + \mathbf{w}, \tag{1}$$

where $\mathbf{x} \in \mathbb{C}^{N_r \times 1}$ is the signal vector, $\mathbf{P} \in \mathbb{C}^{N_t \times N_r}$ is the pre-coding matrix and $\mathbf{w} \in \mathbb{C}^{N_r \times 1}$ is an additive white Gaussian noise vector with zero mean and covariance matrix $N_0 \mathbf{I}_{N_r}$.

B. GPQSM REVISITED

In the sequel, we introduce the representative pre-coding aided SM scheme, GPQSM, which performs SM on the receive antennas and the in-phase and quadrature parts of the received signal independently [27].

In GPQSM, the limitation of $N_t \geq N_r$ is a prerequisite to ensure the availability of the ZF or MMSE pre-coding. The signal vector $\mathbf{x}$ has a length of N_r and the pre-coding matrix $\mathbf{P}$ based on the ZF or MMSE criterion is given by

$$\mathbf{P}_{ZF} = \mathbf{\Omega H}^H (\mathbf{HH}^H)^{-1}, \tag{2}$$

or

$$\mathbf{P}_{MMSE} = \mathbf{\Omega H}^H (\mathbf{HH}^H + N_0 \mathbf{I}_{N_r})^{-1}, \tag{3}$$

respectively, where $\mathbf{\Omega} = \mathrm{diag}\{\omega_1, \omega_2, \ldots, \omega_{N_r}\}$ is the normalizing diagonal matrix. To ensure a constant instantaneous transmit power, the diagonal elements can be chosen as $\omega_i = 1/\sqrt{||\mathbf{p}_i||^2}$, $i = 1, 2, \ldots, N_r$, where $\mathbf{p}_i$ denotes the i-th

column of $\mathbf{P}_{ZF}$ or $\mathbf{P}_{MMSE}$ for ZF or MMSE pre-coding, respectively. Take ZF precoding as an example. The received signal vector can be expressed from (1) and (2) as

$$\mathbf{y} = \mathbf{\Omega}\mathbf{x} + \mathbf{w}, \tag{4}$$

which implies that the ICI is completely eliminated and N_r parallel channels with fading coefficients $\{\omega_1, \omega_2, \ldots, \omega_{N_r}\}$ are resulted. On the other hand, we can also set the average transmit power to be constant, in which case the normalizing diagonal matrix becomes $\mathbf{\Omega} = \sqrt{N_t/\mathrm{Tr}\{(\mathbf{H}^H\mathbf{H})^{-1}\}}\mathbf{I}_{N_r}$. From above, it can be readily figured out that by applying either the instantaneous transmit power constraint or the average transmit power constraint, the resulting parallel channels are highly correlated with each other. The correlated channels significantly degrade the system performance, as will be verified in Section V.

III. PROPOSED VSM

To avoid the high channel correlation resulting from the ZF pre-coding or MMSE pre-coding, we propose a novel pre-coding scheme, i.e., the VSM scheme.

A. PRINCIPLE OF VSM

The well-known parallel decomposition of $\mathbf{H}$ using SVD is given by

$$\mathbf{H} = \mathbf{U}\mathbf{\Sigma}\mathbf{V}^H, \tag{5}$$

where $\mathbf{U} \in \mathbb{C}^{N_r \times N_r}$ and $\mathbf{V} \in \mathbb{C}^{N_t \times N_t}$ are unitary matrices and $\mathbf{\Sigma} \in \mathbb{C}^{N_r \times N_t}$ is the singular value matrix. Inspired by SVD, we aim to transmit the spatial bits through the virtual parallel channels in $\mathbf{\Sigma}$. If we have perfect channel estimation at the receiver and perfect feedback of the CSI from the receiver to the transmitter, the pre-coding matrix can be simply obtained from $\mathbf{V}$. However, the assumption never holds in practical systems. Therefore, to be practical we take into account the imperfect channel estimation and limited feedback in this paper. Note that the receiver uses the orthogonal pilots to estimate the CSI and the maximum-likelihood (ML) channel estimation is employed at the receiver. Therefore, the resulting estimated channel with errors at the receiver can be modeled as [34], [35]

$$\tilde{\mathbf{H}} = \mathbf{H} + \mathbf{H}_e, \tag{6}$$

where $\mathbf{H}_e$ denotes the channel estimation error matrix whose entries are independent and identically distributed (i.i.d.) complex Gaussian RVs with zero mean and variance δ_e^2. Note that $\mathbf{H}_e$ is independent of $\mathbf{H}$ and $\tilde{\mathbf{H}}$ depends on $\mathbf{H}$ with the correlation coefficient $\rho = 1/(1+\delta_e^2)$. It can be seen that $\delta_e^2 = 0$ indicates a special case of the channel estimation without errors. Based on the first-order autoregressive model, we have

$$\mathbf{H} = \rho\tilde{\mathbf{H}} + \mathbf{G}, \tag{7}$$

where $\mathbf{G} \in \mathbb{C}^{N_r \times N_t}$ is a complex Gaussian matrix independent of $\tilde{\mathbf{H}}$, whose entries have zero mean and variance $(1-\rho)$. According to $\tilde{\mathbf{H}}$, the limited feedback channel $\bar{\mathbf{H}}$ is given by CSI quantization [36]

$$\tilde{\mathbf{H}} = \bar{\mathbf{H}} + \mathbf{E}_F, \tag{8}$$

where $\mathbf{E}_F \in \mathbb{C}^{N_r \times N_t}$ denotes a noise matrix independent of $\bar{\mathbf{H}}$, whose entries are i.i.d. complex Gaussian RVs with zero mean and variance δ_F^2. Here, δ_F^2 represents the average channel quantization distortion. Note that $\delta_F^2 = 0$ indicates the channel quantization without distortion. Since $\mathbf{G}$, $\mathbf{E}_F$ and $\bar{\mathbf{H}}$ are independent with each other, the true channel matrix can be expressed through the limited feedback channel by substituting (8) into (7) as

$$\mathbf{H} = \rho\bar{\mathbf{H}} + \mathbf{\Psi}, \tag{9}$$

where $\mathbf{\Psi} \in \mathbb{C}^{N_r \times N_t}$ is the corresponding noise matrix whose entries are i.i.d. complex Gaussian RVs with zero mean and variance $\rho^2\delta_F^2 + (1-\rho)$. From (9), we can see that the effects of the channel estimation and limited feedback channel are incorporated into $\mathbf{\Psi}$. Therefore, for simplicity, it is advisable to attribute the effect of the limited feedback channel to the imperfect channel estimation and only consider the impact of the imperfect channel estimation ($\tilde{\mathbf{H}} = \bar{\mathbf{H}}$ with $\delta_F^2 = 0$). In this paper, the value of ρ is chosen according to two different criterions: (1) fixed ρ: the value of estimation error is fixed for all SNRs; (2) unfixed ρ: the estimation error changes with the given SNR as $\delta_e^2 = 1/(l\gamma)$, where $\gamma = 1/N_0$ denotes the SNR and l denotes the number of pilot symbols used for channel estimation [37].

Due to the channel estimation, the receiver knows $\tilde{\mathbf{H}}$ instead of $\mathbf{H}$. Performing SVD to $\tilde{\mathbf{H}}$, we have

$$\tilde{\mathbf{H}} = \tilde{\mathbf{U}}\tilde{\mathbf{\Sigma}}\tilde{\mathbf{V}}^H, \tag{10}$$

where $\tilde{\mathbf{U}} \in \mathbb{C}^{N_r \times N_r}$ and $\tilde{\mathbf{V}} \in \mathbb{C}^{N_t \times N_t}$ are unitary matrices and $\tilde{\mathbf{\Sigma}} \in \mathbb{C}^{N_r \times N_t}$ is the singular value matrix. Under the assumptions of $N_t \geq N_r$ and a rich scattering environment, $\tilde{\mathbf{\Sigma}} \in \mathbb{C}^{N_r \times N_t}$ contains non-zero singular values $\{\tilde{\sigma}_i\}_{i=1}^{N_r}$, which provide N_r virtual parallel channels to carry spatial bits. Therefore, the SVD of $\tilde{\mathbf{H}}$ in (10) can be rewritten as

$$\tilde{\mathbf{H}} = \tilde{\mathbf{U}}[\tilde{\mathbf{\Sigma}}_1, \mathbf{0}][\tilde{\mathbf{V}}_1, \tilde{\mathbf{V}}_0]^H = \tilde{\mathbf{U}}\tilde{\mathbf{\Sigma}}_1\tilde{\mathbf{V}}_1^H, \tag{11}$$

where $\tilde{\mathbf{\Sigma}}_1 \in \mathbb{C}^{N_r \times N_r}$ is a diagonal matrix whose diagonal elements are $\{\tilde{\sigma}_i\}_{i=1}^{N_r}$, $\tilde{\mathbf{V}}_1 \in \mathbb{C}^{N_t \times N_r}$ and $\tilde{\mathbf{V}}_0 \in \mathbb{C}^{N_t \times (N_t - N_r)}$ are sub-matrices of $\tilde{\mathbf{V}}$, which contain N_r right-singular vectors corresponding to nonzero singular values and $N_t - N_r$ right-singular vectors corresponding to zero singular values, respectively. From (11), the signal vector can be set as $\mathbf{x} \in \mathbb{C}^{N_r \times 1}$, and $\tilde{\mathbf{V}}_1$ is fed back to the transmitter for pre-coding purpose.

B. VSM TRANSMITTER

The transmitter structure of VSM is depicted in Fig. 1. In VSM, N_p out of N_r virtual parallel channels are activated to transmit the real (imaginary) parts of the modulated symbols. In order to modulate the information bits, only $N = 2^{\lfloor \log_2(\mathrm{C}(N_r, N_p)) \rfloor}$ combinations are selected as the legitimate

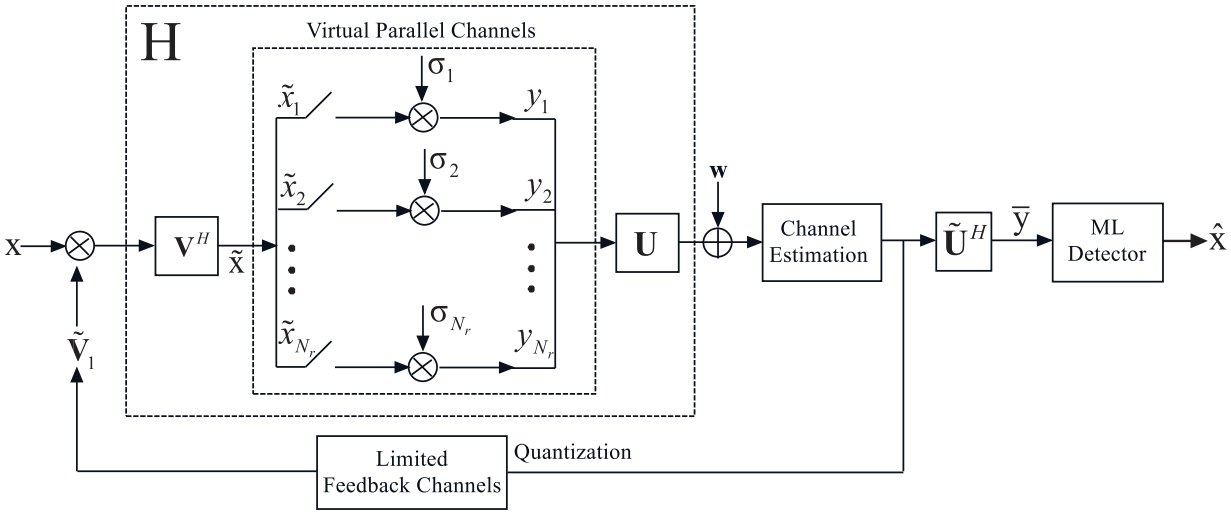

FIGURE 1. The schematic of VSM.

antenna combinations. Specifically, VSM works as follows. At each time slot, $d = N_p \log_2(M) + 2\lfloor \log_2(\mathrm{C}(N_r, N_p)) \rfloor$ information bits are divided into three parts. The first part of $N_p \log_2(M)$ bits are mapped into a symbol vector $\mathbf{s} = [s_1, \ldots, s_{N_p}]^T$, where $s_\varphi = s_\varphi^I + j s_\varphi^Q$, $\varphi \in \{1, \ldots, N_p\}$, with s_φ^I and s_φ^Q denoting the in-phase and quadrature parts of s_φ, respectively. Note that $s_\varphi^I \in \mathcal{S}^I$ and $s_\varphi^Q \in \mathcal{S}^Q$, where $\mathcal{S}^I$ and $\mathcal{S}^Q$ denote the in-phase and quadrature sets of $\mathcal{S}$, respectively. The second part of $\lfloor \log_2(\mathrm{C}(N_r, N_p)) \rfloor$ bits select an active channel combination $I_v^I = \{i_v^I(1), \ldots, i_v^I(N_p)\}$, where $i_v^I(\alpha) \in \{1, \ldots N_r\}$ with $v \in \{1, \ldots, N\}$ and $\alpha \in \{1, \ldots, N_p\}$, to transmit the real part of $\mathbf{s}$, yielding $\mathbf{x}^I = [\ldots, s_1^I, \ldots, s_{N_p}^I, \ldots]$. Similarly, the third part of $\lfloor \log_2(\mathrm{C}(N_r, N_p)) \rfloor$ bits select an active channel combination $I_\mu^Q = \{i_\mu^Q(1), \ldots, i_\mu^Q(N_p)\}$, where $i_\mu^Q(\varsigma) \in \{1, \ldots N_r\}$ with $\mu \in \{1, \ldots, N\}$ and $\varsigma \in \{1, \ldots, N_p\}$, to transmit the imaginary part of $\mathbf{s}$, yielding $\mathbf{x}^Q = [\ldots, s_1^Q, \ldots, s_{N_p}^Q, \ldots]$. Finally, the information vector is generated by combining the in-phase and quadrature parts:

$$\mathbf{x} = \mathbf{x}^I + j\mathbf{x}^Q. \tag{12}$$

As an example, we present a mapping table of VSM for $N_t = 4$, $N_r = 2$, $N_p = 1$ and 4-QAM in Table I. In this example, we have $d = 4$. Suppose that the information bits $q = [0\ 1\ 1\ 0]$ are transmitted at a given time slot. The first $N_p \log_2(M) = 2$ bits $[0\ 1]$ are mapped into $\mathbf{s} = [-1-j]$. Then, $\mathbf{s}$ is divided into in-phase and quadrature parts $\mathbf{s}^I = [-1]$ and $\mathbf{s}^Q = [-1]$, respectively. The second $\lfloor \log_2(\mathrm{C}(N_r, N_p)) \rfloor = 1$ bit $[1]$ indicates that the active channel combination $I_2^I = \{2\}$ is chosen to transmit $\mathbf{s}^I$, resulting in the vector $\mathbf{x}^I = [0, -1]^T$. The last $\lfloor \log_2(\mathrm{C}(N_r, N_p)) \rfloor = 1$ bit $[0]$ indicates to select the active channel combination $I_1^Q = \{1\}$ to transmit $\mathbf{s}^Q$, which results in the vector $\mathbf{x}^Q = [1, 0]^T$. Finally, the information vector is obtained as $\mathbf{x} = [-j, -1]^T$.

Input bits	Signal vector	Input bits	Signal vector
0000	$[-1+j, 0]^T$	1000	$[1+j, 0]^T$
0001	$[-1, j]^T$	1001	$[1, j]^T$
0010	$[j, -1]^T$	1010	$[j, 1]^T$
0011	$[0, -1+j]^T$	1011	$[0, 1+j]^T$
0100	$[-1-j, 0]^T$	1100	$[1-j, 0]^T$
0101	$[-1, -j]^T$	1101	$[1, -j]^T$
0110	$[-j, -1]^T$	1110	$[-j, 1]^T$
0111	$[0, -1-j]^T$	1111	$[0, 1-j]^T$

TABLE 1. Mapping table for VSM with $N_t = 4$, $N_r = 2$, $N_p = 1$ and 4-QAM.

Before transmitted into the wireless channel, the information vector is pre-coded by $\mathbf{P} = \tilde{\mathbf{V}}_1$.

C. VSM RECEIVER

The receiver structure of VSM is depicted in Fig.1. The received signal vector after receiver shaping can be expressed as

$$\bar{\mathbf{y}} = \tilde{\mathbf{U}}^H \mathbf{y} = \tilde{\mathbf{U}}^H \mathbf{H} \tilde{\mathbf{V}}_1 \mathbf{x} + \tilde{\mathbf{U}}^H \mathbf{w}. \tag{13}$$

Based on (13), we propose two detection methods corresponding to whether or not the receiver has the knowledge of the correlation coefficient ρ. When ρ is known to the receiver, the maximum-likelihood (ML) detector can be derived as

$$\hat{\mathbf{x}} = \arg\min_{\mathbf{x}} \|\bar{\mathbf{y}} - \rho \tilde{\mathbf{\Sigma}}_1 \mathbf{x}\|^2. \tag{14}$$

On the other hand, when ρ is unknown to the receiver, it is reasonable to assume perfect channel estimation for detection and thus the detector follows from (14) by setting $\rho = 1$:

$$\hat{\mathbf{x}} = \arg\min_{\mathbf{x}} \|\bar{\mathbf{y}} - \tilde{\mathbf{\Sigma}}_1 \mathbf{x}\|^2. \tag{15}$$

However, both receivers in (14) and (15) impose great computational burden to the receiver when N_r or M goes to a very large value. To solve this problem, inspired by [27] we further propose a low-complexity detector in the following.

For brevity, we only consider the detection with ρ unknown to the receiver. In light of (12), we can rewrite (15) as

$$\hat{\mathbf{x}} = \arg\min_{\mathbf{x}^I} \|\bar{\mathbf{y}}^I - \tilde{\mathbf{\Sigma}}_1 \mathbf{x}^I\|^2 + j \arg\min_{\mathbf{x}^Q} \|\bar{\mathbf{y}}^Q - \tilde{\mathbf{\Sigma}}_1 \mathbf{x}^Q\|^2, \tag{16}$$

where $\bar{\mathbf{y}}^I$ and $\bar{\mathbf{y}}^Q$ denote the real and imaginary parts of $\bar{\mathbf{y}}$, respectively. Due to the independence between the real and imaginary parts of $\mathbf{x}$, the detections for the real and imaginary parts can be performed independently. Without loss of generality, we only consider the detection for the real part, which can be expressed as

$$\begin{aligned}
\hat{\mathbf{x}}^I &= \arg\min_{\mathbf{x}^I} \|\bar{\mathbf{y}}^I - \tilde{\mathbf{\Sigma}}_1 \mathbf{x}^I\|^2 \\
&= \arg\min_{\{x_i^I\}_{i=1}^{N_r}} \sum_{i=1}^{N_r} |\bar{y}_i^I - \tilde{\sigma}_i x_i^I|^2 \\
&= \arg\min_{\{x_i^I\}_{i=1}^{N_r}} \sum_{i=1}^{N_r} \left[\left(\bar{y}_i^I\right)^2 - 2\tilde{\sigma}_i x_i^I \bar{y}_i^I + \left(\tilde{\sigma}_i x_i^I\right)^2 \right] \\
&= \arg\min_{I_v^I} \sum_{i \in I_v^I} \min_{s_i^I} \left[\left(\tilde{\sigma}_i s_i^I\right)^2 - 2\tilde{\sigma}_i s_i^I \bar{y}_i^I \right].
\end{aligned} \tag{17}$$

Denote $D_i = \left(\tilde{\sigma}_i \hat{s}_i^I\right)^2 - 2\tilde{\sigma}_i \hat{s}_i^I \bar{y}_i^I$ and

$$\hat{s}_i^I = \arg\min_{s \in \mathcal{S}^I} |\bar{y}_i^I - \tilde{\sigma}_i s|^2, \tag{18}$$

which represents the hard decision on $\bar{y}_i^I$. The detection for the active channel combination (legitimate channel combination) in (17) is thus equivalent to

$$\hat{I}_v^I = \arg\min_{I_v^I} \sum_{i \in I_v^I} D_i. \tag{19}$$

It is clear that the order of the search complexity in (19) is $N_r M^I + N$, where M^I denotes the cardinality of $\mathcal{S}^I$. However, the search complexity is still high especially when N_r or N_p is large. To further reduce the search complexity, it is advisable to select active channel combination via $[z_1, \ldots, z_{N_r}] = \text{sort}(\{D_i\}_{i=1}^{N_r})$, where z_1 and z_{N_r} are the indices of the maximum and minimum values in $\{D_i\}_{i=1}^{N_r}$, respectively. Therefore, we can simply obtain the active channel combination by $\hat{I}_v^I = \text{sort}([z_1, \ldots, z_{N_p}])$. In this manner, however, we may obtain an illegitimate channel combination, which does not exist in the mapping table. To relieve this adverse effect, when this event occurs, we select $\hat{I}_v^I = \text{sort}([z_1, \ldots, z_{N_{p-1}}, z_{N_{p+1}}])$ instead, which is the second most likely to happen. Note that if the alternative channel combination is still illegal, we simply set the estimated information bits to be all 0 bits. After getting $\hat{I}_v^I$, the estimation of $\mathbf{x}^I$ is directly obtained by

$$\hat{x}_i^I = \begin{cases} \hat{s}_i^I, & i \in \hat{I}_v^I \\ 0, & \text{otherwise.} \end{cases} \tag{20}$$

From above, we see that the equivalent detection only leads to a search complexity of order $N_r M^I$. Compared with (15), the search complexity is largely reduced.

IV. PERFORMANCE ANALYSIS

In this section, we analytically derive the ABEP of VSM for the ML detection in (14). To study the diversity order and coding gain, we further derive the asymptotic ABEP of VSM. The provided results, as will be verified in Section V, is also valid for the ML detection in (15).

A. ANALYSIS OF ABEP

According to (7), $\bar{\mathbf{y}}$ can be rewritten from (13) as

$$\bar{\mathbf{y}} = \rho \tilde{\mathbf{\Sigma}}_1 \mathbf{x} + \mathbf{q}, \tag{21}$$

where $\mathbf{q} = \tilde{\mathbf{U}}^H \mathbf{G} \tilde{\mathbf{V}}_1 \mathbf{x} + \tilde{\mathbf{U}}^H \mathbf{w}$. Since multiplying a matrix by any unitary matrix does not change the probability distribution, we can conclude that $\tilde{\mathbf{U}}^H \mathbf{G} \tilde{\mathbf{V}}_1$ and $\tilde{\mathbf{U}}^H \mathbf{w}$ have the same distribution as $\mathbf{G}$ and $\mathbf{w}$, respectively. In addition, since $\mathbf{G}$ and $\mathbf{w}$ are mutually independent, each entry of $\mathbf{q}$ follows the complex Gaussian distribution with zero mean and variance

$$\psi = N_0 + (1 - \rho)||\mathbf{x}||^2. \tag{22}$$

At this point, it is straightforward to arrive at (14) or (15) from (21) for detection.

Denote $\mathbf{c} \triangleq [c_1, \ldots, c_{N_r}]^T = \mathbf{x} - \hat{\mathbf{x}}$. In light of (15) and (21), the average PEP of detecting $\hat{\mathbf{x}}$ when $\mathbf{x}$ is transmitted on $\tilde{\mathbf{\Sigma}}_1$ can be calculated as

$$\begin{aligned}
&\Pr(\mathbf{x} \to \hat{\mathbf{x}}|\tilde{\mathbf{\Sigma}}_1) \\
&= \Pr(||\bar{\mathbf{y}} - \tilde{\mathbf{\Sigma}}_1 \mathbf{x}||^2 > ||\bar{\mathbf{y}} - \tilde{\mathbf{\Sigma}}_1 \hat{\mathbf{x}}||^2) \\
&= Q\left(\sqrt{\frac{||\rho \tilde{\mathbf{\Sigma}}_1 (\mathbf{x} - \hat{\mathbf{x}})||^2}{2\psi}} - (1 - \rho) \frac{||\tilde{\mathbf{\Sigma}}_1 \mathbf{x}||^2 - ||\tilde{\mathbf{\Sigma}}_1 \hat{\mathbf{x}}||^2}{\sqrt{2\psi ||\tilde{\mathbf{\Sigma}}_1 (\mathbf{x} - \hat{\mathbf{x}})||^2}} \right).
\end{aligned} \tag{23}$$

However, averaging (23) is nearly unavailable due to the difficulty in obtaining the exact PDF of the second part in Q-function. Therefore, it may be difficult to obtain closed-form upper-bounded and asymptotic ABEPs of VSM that adopts the receiver in (15). Alternatively, we resorts to (14) for the derivation of PEP in this paper. In light of (14) and (21), the average PEP can be calculated as

$$\begin{aligned}
&\Pr(\mathbf{x} \to \hat{\mathbf{x}}|\tilde{\mathbf{\Sigma}}_1) \\
&= \Pr(||\bar{\mathbf{y}} - \rho \tilde{\mathbf{\Sigma}}_1 \mathbf{x}||^2 > ||\bar{\mathbf{y}} - \rho \tilde{\mathbf{\Sigma}}_1 \hat{\mathbf{x}}||^2) \\
&= Q\left(\sqrt{\frac{||\rho \tilde{\mathbf{\Sigma}}_1 (\mathbf{x} - \hat{\mathbf{x}})||^2}{2\psi}} \right) \\
&= Q\left(\sqrt{\frac{\sum_{i=1}^{N_r} \lambda_i |c_i|^2}{2\psi}} \right),
\end{aligned} \tag{24}$$

where $\lambda_i = \rho^2 \tilde{\sigma}_i^2$, $i \in \{1, \ldots, N_r\}$.

From (24), it can be seen that the derivation of PEP needs the joint PDF of $\mathbf{\Lambda} = [\lambda_1, \ldots, \lambda_{N_r}]^T$, which is given by [38]

$$f(\mathbf{\Lambda}) = \frac{1}{K} e^{-\sum_{i=1}^{N_r} \lambda_i} \underbrace{\prod_{i=1}^{N_r} \lambda_i^{N_t - N_r} \prod_{j=i+1}^{N_r} (\lambda_i - \lambda_j)^2}_{\Upsilon}$$
$$= \frac{1}{K} \sum_{\kappa=1}^{L} a_\kappa e^{-\sum_{i=1}^{N_r} \lambda_i} \lambda_1^{b_\kappa^1} \cdots \lambda_{N_r}^{b_\kappa^{N_r}}, \quad (25)$$

where K is a normalizing coefficient, L denotes the number of monomials in Υ, a_κ denotes the coefficient of the κ-th monomial in Υ with $\kappa \in \{1, \ldots L\}$ and $\{b_\kappa^i\}_{i=1}^{N_r}$ denote the power coefficients of $\{\lambda_i\}_{i=1}^{N_r}$ in the κ-th monomial in Υ. An example for all values of $(K, a_\kappa, b_\kappa^1, \ldots, b_\kappa^{N_r})$ with $N_t = 4$ and $N_r = 3$ is given in Table 2. By averaging (24) with (25), we have

$$\Pr(\mathbf{x} \to \hat{\mathbf{x}}) = E_{\mathbf{\Lambda}} \left[Q\left(\sqrt{\frac{\sum_{i=1}^{N_r} \lambda_i |c_i|^2}{2\psi}} \right) \right]$$
$$\cong E_{\mathbf{\Lambda}} \left[\frac{1}{12} e^{-\sum_{i=1}^{N_r} \frac{\lambda_i |c_i|^2}{4\psi}} + \frac{1}{4} e^{-\sum_{i=1}^{N_r} \frac{\lambda_i |c_i|^2}{3\psi}} \right] \quad (26)$$
$$= \frac{1}{12} \int e^{-\sum_{i=1}^{N_r} \frac{\lambda_i |c_i|^2}{4\psi}} f(\mathbf{\Lambda}) d\mathbf{\Lambda}$$
$$+ \frac{1}{4} \int e^{-\sum_{i=1}^{N_r} \frac{\lambda_i |c_i|^2}{3\psi}} f(\mathbf{\Lambda}) d\mathbf{\Lambda}, \quad (27)$$

where (26) is obtained by [39]

$$Q(x) \cong \frac{1}{12} e^{-\frac{x^2}{2}} + \frac{1}{4} e^{-\frac{2x^2}{3}}. \quad (28)$$

According to [33, eq. (8.312.2)], the first integral of (27) can be calculated as

$$\frac{1}{12} \int e^{\frac{-\sum_{i=1}^{N_r} \lambda_i |c_i|^2}{4\psi}} f(\mathbf{\Lambda}) d\mathbf{\Lambda}$$
$$= \frac{1}{12K} \sum_{\kappa=1}^{L} a_\kappa \int e^{-\sum_{i=1}^{N_r} (\frac{|c_i|^2}{4\psi} + 1)\lambda_i} \lambda_1^{b_\kappa^1} \cdots \lambda_{N_r}^{b_\kappa^{N_r}} d\mathbf{\Lambda}$$
$$= \frac{1}{12K} \sum_{\kappa=1}^{L} a_\kappa \int e^{-(\frac{|c_1|^2}{4\psi} + 1)\lambda_1} \lambda_1^{b_\kappa^1} d\lambda_1$$
$$\times \cdots \times \int e^{-(\frac{|c_{N_r}|^2}{4\psi} + 1)\lambda_{N_r}} \lambda_{N_r}^{b_\kappa^{N_r}} d\lambda_{N_r}$$
$$= \frac{1}{12K} \sum_{\kappa=1}^{L} a_\kappa \prod_{i=1}^{N_r} \left(\frac{|c_i|^2}{4\psi} + 1 \right)^{-(b_\kappa^i + 1)} \Gamma(b_\kappa^i + 1). \quad (29)$$

In the same manner, the second integral of (27) is given by

$$\frac{1}{4} \int e^{-\sum_{i=1}^{N_r} \frac{\lambda_i |c_i|^2}{3\psi}} f(\mathbf{\Lambda}) d\mathbf{\Lambda}$$
$$= \frac{1}{4K} \sum_{\kappa=1}^{L} a_\kappa \prod_{i=1}^{N_r} \left(\frac{|c_i|^2}{3\psi} + 1 \right)^{-(b_\kappa^i + 1)} \Gamma(b_\kappa^i + 1). \quad (30)$$

By substituting (29) and (30) into (27), the unconditional PEP can be expressed as

$$\Pr(\mathbf{x} \to \hat{\mathbf{x}}) = \frac{1}{4K} \sum_{\kappa=1}^{L} a_\kappa \left(\prod_{i=1}^{N_r} \Gamma(b_\kappa^i + 1) \right)$$
$$\times \left[\frac{1}{3} \prod_{i=1}^{N_r} \left(\frac{|c_i|^2}{4\psi} + 1 \right)^{-(b_\kappa^i + 1)} \right.$$
$$\left. + \prod_{i=1}^{N_r} \left(\frac{|c_i|^2}{3\psi} + 1 \right)^{-(b_\kappa^i + 1)} \right]. \quad (31)$$

After obtaining the PEP, an upper bound on the ABEP can be readily derived according to the union bounding technique as [40]

$$P_e \le \frac{1}{d 2^d} \sum_{\mathbf{x}} \sum_{\hat{\mathbf{x}} \ne \mathbf{x}} N(\mathbf{x} \to \hat{\mathbf{x}}) \Pr(\mathbf{x} \to \hat{\mathbf{x}}), \quad (32)$$

where $N(\mathbf{x} \to \hat{\mathbf{x}})$ measures the number of bits in error between $\mathbf{x}$ and $\hat{\mathbf{x}}$.

B. ASYMPTOTIC ABEP ANALYSIS

Recall $\psi = N_0 + (1-\rho)||\mathbf{x}||^2$. If we have channel estimation error ($\rho \ne 1$), $N_0 = 1/\gamma$ tends to be zero and $\psi \to \psi^* = (1-\rho)||\mathbf{x}||^2$ as $\gamma \to +\infty$. By substituting (31) into (32) with $\psi = \psi^*$, the asymptotic ABEP can be thus expressed as

$$P_e \to \frac{1}{d 2^{d+2} K} \sum_{\mathbf{x}} \sum_{\hat{\mathbf{x}}} N(\mathbf{x} \to \hat{\mathbf{x}}) \sum_{\kappa=1}^{L} a_\kappa \left(\prod_{i=1}^{N_r} \Gamma(b_\kappa^i + 1) \right)$$
$$\times \left[\frac{1}{3} \prod_{i=1}^{N_r} \left(\frac{|c_i|^2}{4\psi^*} + 1 \right)^{-(b_\kappa^i + 1)} \right.$$
$$\left. + \prod_{i=1}^{N_r} \left(\frac{|c_i|^2}{3\psi^*} + 1 \right)^{-(b_\kappa^i + 1)} \right]. \quad (33)$$

The above equation reveals that the ABEP tends to be a constant irrelevant to the SNR in the high SNR region, which, as reflected in the ABEP performance, creates an error floor.

On the other hand, if no channel estimation error exists ($\rho = 1$), we have $\psi = 1/\gamma$ and the asymptotic ABEP can be derived as

$$P_e \to \frac{1}{d 2^{d+2} K} \sum_{\mathbf{x}} \sum_{\hat{\mathbf{x}}} N(\mathbf{x} \to \hat{\mathbf{x}}) \sum_{\kappa=1}^{L} a_\kappa \left(\prod_{i=1}^{N_r} \Gamma(b_\kappa^i + 1) \right)$$
$$\times \left[\frac{1}{3} \prod_{i=1}^{N_r} \left(\frac{|c_i|^2 \gamma}{4} \right)^{-(b_\kappa^i + 1)} + \prod_{i=1}^{N_r} \left(\frac{|c_i|^2 \gamma}{3} \right)^{-(b_\kappa^i + 1)} \right]. \quad (34)$$

From (34), we see that the high SNR approximation of P_e turns out to be a linear combination of PEPs, which are

κ	a_κ	b_κ^1	b_κ^2	b_κ^3	κ	a_κ	b_κ^1	b_κ^2	b_κ^3
1	1	1	3	5	11	2	3	2	4
2	-2	1	4	4	12	2	4	2	3
3	1	1	5	3	13	2	4	3	2
4	2	2	3	4	14	-2	4	4	1
5	2	2	4	3	15	1	3	1	5
6	-2	2	5	2	16	-2	4	1	4
7	-6	3	3	3	17	1	5	1	3
8	2	3	4	2	18	-2	5	2	2
9	1	3	5	1	19	1	5	3	1
10	-2	2	2	5					

TABLE 2. A look-up table for $N_t = 4$, $N_r = 3$ ($K = 144$).

dominated by the sum of the terms associated with the largest exponent (equivalently the smallest value among $\{b_\kappa^i\}_{i=1}^{N_r}$ for all κ(s) of γ. For instance, from Table 2 with $N_t = 4$ and $N_r = 3$, the smallest coefficient is 1. From the above analysis, the asymptotic ABEP in (34) can be further approximated as

$$P_e \to \frac{\gamma^{-d_{min}}}{d 2^{d+2} K} \sum_{\kappa, d_{min}} \sum_{s,\hat{s}\in\mathcal{S}} a_\kappa \left(\prod_{i=1}^{N_r} \Gamma(b_\kappa^i + 1) \right) N(\mathbf{x} \to \hat{\mathbf{x}}) \times \left(\frac{|s-\hat{s}|^{-2d_{min}}}{3 \cdot 4^{-d_{min}}} + \frac{|s-\hat{s}|^{-2d_{min}}}{3^{-d_{min}}} \right), \quad (35)$$

where $d_{min} = N_t - N_r + 1$ is the diversity order achieved by the VSM scheme and $\sum_{\kappa, d_{min}}$ denotes the sum applying to all κ(s) for which there exists the coefficient d_{min}. From (35), we see that similar to the existing pre-coding schemes, the diversity order of VSM is determined by the configuration of the transceiver antennas only and is irreverent to N_p. By definition [41], the coding gain achieved by the VSM scheme can be derived from (35) as

$$G_c = \left[\frac{1}{K d 2^{d+2}} \sum_{\kappa, d_{min}} \sum_{s,\hat{s}\in\mathcal{S}} a_\kappa \left(\prod_{i=1}^{N_r} \Gamma(b_\kappa^i + 1) \right) N(\mathbf{x} \to \hat{\mathbf{x}}) \times \left(\frac{|s-\hat{s}|^{-2d_{min}}}{3 \cdot 4^{-d_{min}}} + \frac{|s-\hat{s}|^{-2d_{min}}}{3^{-d_{min}}} \right) \right]^{-\frac{1}{d_{min}}}, \quad (36)$$

which satisfies

$$P_e \cong (G_c \gamma)^{-d_{min}}, \quad (37)$$

in the high SNR region.

V. SIMULATION RESULTS AND ANALYSIS

We conduct computer simulations to evaluate the ABEP performance of VSM. The 4QAM constellation is assumed for all schemes.

A. PERFORMANCE COMPARISON WITH GPQSM

We compare the ABEP performance of VSM with that of GPQSM in Figs. 2 and 3. The simulation parameters for Fig. 2

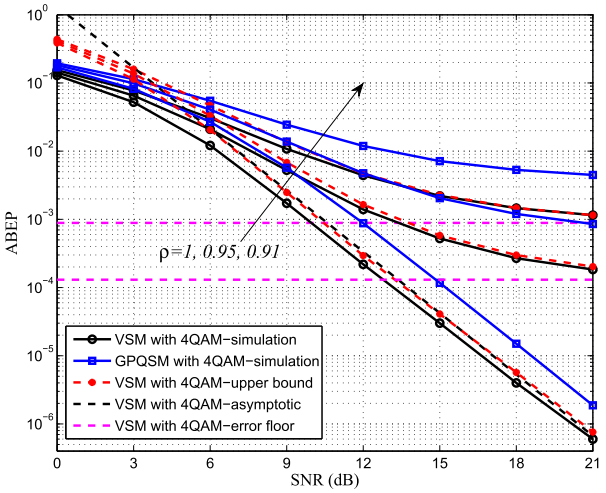

FIGURE 2. Comparison between VSM and GPQSM in terms of ABEP with $\rho = 1, 0.95, 0.91$ for $N_t = 4$, $N_r = 2$ and $N_p = 1$.

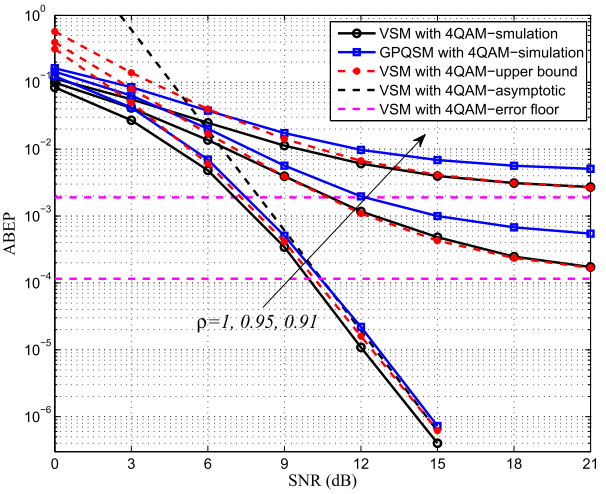

FIGURE 3. Comparison between VSM and GPQSM in terms of ABEP with $\rho = 1, 0.95, 0.91$ for $N_t = 8$, $N_r = 4$ and $N_p = 2$.

are chosen as $N_t = 4, N_r = 2$ and $N_p = 1$, and those for Fig. 3 are $N_t = 8$, $N_r = 4$ and $N_p = 2$. Since the proposed low-complexity detector achieves almost the same performance as the ML detector, we have removed its ABEP curves for figure clarity. To examine the effect of channel estimation, we consider $\rho = 1$, 0.95, and 0.91, which correspond to $\delta_e^2 = 0$, 0.05, and 0.1, respectively. To verify our analysis, the analytical ABEP upper bounds and asymptotic results of VSM are also added in the figures. It is observed from Figs. 2 and 3 that, similar to GPQSM, under imperfect channel estimation, VSM results in error floors, whose levels are accurately characterized by the analytical results. In addition, the error floor increases with the channel estimation error, applying to both schemes. However, the floor level for VSM is much lower. The above observation can be explained by (21), which reveals that the power of the equivalent noise $\mathbf{q}$ scales with the channel estimation error rather than the SNR.

On the other hand, under perfect channel estimation, VSM archives a diversity order of $N_t - N_r + 1$ as GPQSM while obtaining a much larger coding gain. For example, as seen from Fig. 2, about 2dB SNR gain is obtained at an ABEP value of 10^{-5}. This superiority can be accounted for the more diverse parallel channels resulted from the SVD.

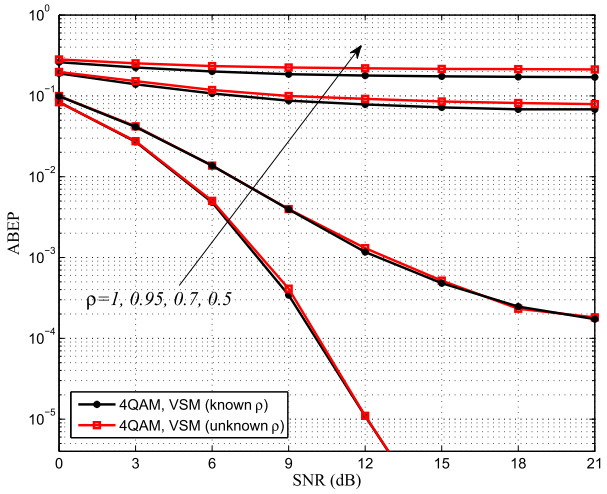

FIGURE 4. Comparison of the performances of VSM receivers (14) and (15) in terms of ABEP with $\rho = 1, 0.95, 0.7, 0.5$ for $N_t = 8$, $N_r = 4$ and $N_p = 2$.

B. IMPACT OF ρ ON PERFORMANCE

We examine the impact of the knowledge of ρ to the receiver on the performance of VSM systems. Fig. 4 shows the comparison results between the ABEPs of the receivers (14) and (15) with the fixed $\rho = 1, 0.95, 0.7, 0.5$ for $N_t = 8$, $N_r = 4$ and $N_p = 2$. From the figure, we see that for large correlation coefficients such as $\rho = 1$ and 0.95, nearly the same performance is resulted no matter whether ρ is known to the receiver or not. For smaller correlation coefficients such as $\rho = 0.7, 0.5$, the performance with the knowledge of ρ to the receiver is superior to that without the knowledge of ρ. This can be easily understood since the influence of channel estimation becomes more significant as ρ becomes smaller and the knowledge of ρ helps the receiver tract the true channel more accurately. However, we note that as the performance gap becomes apparent, the ABEP value also goes very large, e.g., of the order of 10^{-1} for $\rho = 0.7, 0.5$, which is intolerable for most applications of wireless communications. Therefore, in practice the receiver (15) is preferred for VSM systems in consideration of its simplicity in implementation since usually the true value of ρ is difficult to obtain.

Then, we consider the impact of a different channel estimation model on the ABEP performance of VSM. It is assumed that ρ changes with the SNR according to $\rho = l\gamma/(l\gamma + 1)$, where l is chosen to be 2. Fig. 5 shows the comparison results between performances of VSM and GPQSM with unfixed ρ for two different system configurations, which are 1) $N_t = 4$, $N_r = 2$ and $N_p = 1$; 2) $N_t = 8$, $N_r = 4$ and $N_p = 2$. From

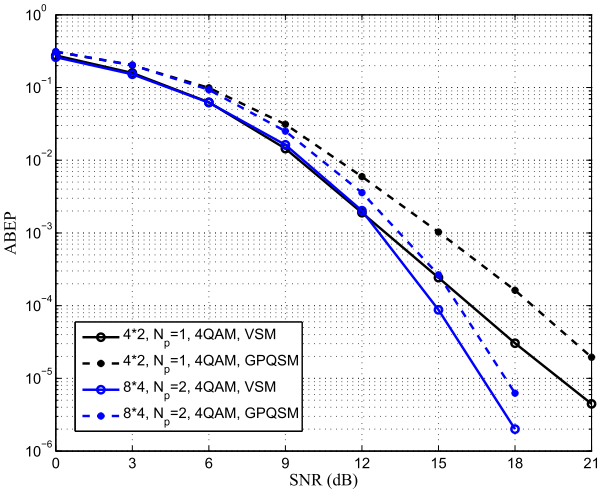

FIGURE 5. Comparison of the performances of VSM and GPQSM in terms of ABEP with unfixed ρ for two different system configurations: 1) $N_t = 4$, $N_r = 2$, and $N_p = 1$; 2) $N_t = 8$, $N_r = 4$, and $N_p = 2$.

the figure, it can be seen that different from what we observe under the situation of fixed ρ, the error floors never appear for both VSM and GPQSM. This is because ρ approaches one, which happens to be the perfect channel estimation case, in the high SNR region. Therefore, the asymptotic results also apply to the situation of unfixed ρ, which are not shown for figure clarity. On the other hand, from Fig. 5, we see that similarly VSM is superior to GPQSM in the whole SNR region.

VI. CONCLUSIONS AND FUTURE WORK

In this paper, we have proposed the VSM scheme, which conveys the spatial bits via the indices of active virtual parallel channels. We have derived closed-form upper bounded and asymptotic ABEPs of VSM with practical channel estimation. The diversity order and coding gain of VSM have also been characterized. Finally, simulation results have shown that the proposed VSM scheme provides a significant performance gain compared with the conventional GPQSM scheme with and without channel estimation errors.

For its nature, VSM also applies to the case of $N_t < N_r$. In this case, VSM performs index modulation on N_t virtual parallel channels, which can be considered as a transmitter-side SM scheme. The performance analysis in this paper is also applicable to VSM for $N_t < N_r$. The potential of VSM as a transmitter-side SM scheme will be studied in the future.

REFERENCES

[1] E. Telatar, "Capacity of multi-antenna Gaussian channels," *Eur. Trans. Telecommun.*, vol. 10, no. 6, pp. 585–595, 1999.
[2] X. Cheng *et al.*, "Communicating in the real world: 3D MIMO," *IEEE Wireless Commun.*, vol. 21, no. 4, pp. 136–144, Aug. 2014.
[3] P. W. Wolniansky, G. J. Foschini, G. D. Golden, and R. A. Valenzuela, "V-BLAST: An architecture for realizing very high data rates over the richscattering wireless channel," in *Proc. URSI Int. Symp. Signal Syst. Electron. ISSSE*, Pisa, Italy, Sep. 1998, pp. 295–300.

[4] V. Tarokh, H. Jafarkhani, and A. R. Calderbank, "Space-time block coding for wireless communications: Performance results," *IEEE J. Sel. Areas Commun.*, vol. 17, no. 3, pp. 451–460, Mar. 1999.

[5] M. Di Renzo, H. Haas, and P. M. Grant, "Spatial modulation for multiple-antenna wireless systems: A survey," *IEEE Commun. Mag.*, vol. 49, no. 12, pp. 182–191, Dec. 2011.

[6] P. Yang, M. Di Renzo, Y. Xiao, S. Li, and L. Hanzo, "Design guidelines for spatial modulation," *IEEE Commun. Surveys Tuts.*, vol. 17, no. 1, pp. 6–26, 1st Quart., 2015.

[7] P. Yang *et al.*, "Single-carrier SM-MIMO: A promising design for broadband large-scale antenna systems," *IEEE Commun. Surveys Tuts.*, vol. 18, no. 3, pp. 1687–1716, 3rd Quart., 2016.

[8] M. Di Renzo, H. Haas, A. Ghrayeb, S. Sugiura, and L. Hanzo, "Spatial modulation for generalized MIMO: Challenges, opportunities, and implementation," *Proc. IEEE*, vol. 102, no. 1, pp. 56–103, Jan. 2014.

[9] A. Younis *et al.*, "Performance of spatial modulation using measured real-world channels," in *Proc. IEEE 78th Veh. Technol. Conf. (VTC Fall)*, Sep. 2013, pp. 1–5.

[10] N. Serafimovski *et al.*, "Practical implementation of spatial modulation," *IEEE Trans. Veh. Technol.*, vol. 62, no. 9, pp. 4511–4523, Nov. 2013.

[11] X. Wu, H. Claussen, M. D. Renzo, and H. Haas, "Channel estimation for spatial modulation," *IEEE Trans. Commun.*, vol. 62, no. 12, pp. 4362–4372, Dec. 2014.

[12] M. Di Renzo, D. De Leonardis, F. Graziosi, and H. Haas, "Space shift keying (SSK—) MIMO with practical channel estimates," *IEEE Trans. Commun.*, vol. 60, no. 4, pp. 998–1012, Apr. 2012.

[13] J. Jeganathan, A. Ghrayeb, L. Szczecinski, and A. Ceron, "Space shift keying modulation for MIMO channels," *IEEE Trans. Wireless Commun.*, vol. 8, no. 7, pp. 3692–3703, Jul. 2009.

[14] J. Jeganathan, A. Ghrayeb, and L. Szczecinski, "Generalized space shift keying modulation for MIMO channels," in *Proc. IEEE 19th Int. Symp. PIMRC*, Cannes, France, Sep. 2008, pp. 1–5.

[15] A. Younis, N. Serafimovski, R. Haas, and H. Haas, "Generalised spatial modulation," in *Proc. Conf. Rec. 44th Asilomer Signals Syst. Comput.*, pp. 1498–1502.

[16] S. Narayanan, M. Di Renzo, F. Graziosi, and H. Haas, "Distributed spatial modulation: A cooperative diversity protocol for half-duplex relay-aided wireless networks," *IEEE Trans. Veh. Technol.*, vol. 65, no. 5, pp. 2947–2964, May 2016.

[17] S. Narayanan, M. Di Renzo, M. J. Chaudhry, F. Graziosi, and H. Haas, "On the achievable performance-complexity tradeoffs of relay-aided space shift keying," *IEEE Trans. Signal Inf. Process. Over Netw.*, vol. 1, no. 2, pp. 129–144, Jun. 2015.

[18] R. C. S. Ikki and H. M. Aggoune, "Quadrature spatial modulation," *IEEE Trans. Veh. Technol.*, vol. 64, no. 6, pp. 2738–2742, Jun. 2015.

[19] R. Mesleh, M. D. Renzo, H. Haas, and P. M. Grant, "Trellis coded spatial modulation," *IEEE Trans. Wireless Commun.*, vol. 9, no. 7, pp. 2349–2361, Jul. 2010.

[20] E. Basar, U. Aygolu, E. Panayirci, and H. V. Poor, "New trellis code design for spatial modulation," *IEEE Trans. Wireless Commun.*, vol. 10, no. 8, pp. 2670–2680, Aug. 2011.

[21] E. Basar, U. Aygolu, E. Panayirci, and H. Poor, "Space-time block coded spatial modulation," *IEEE Trans. Commun.*, vol. 59, no. 3, pp. 823–832, Mar. 2011.

[22] Y. Bian, X. Cheng, M. Wen, L. Yang, H. V. Poor, and B. Jiao, "Differential spatial modulation," *IEEE Trans. Veh. Technol.*, vol. 64, no. 7, pp. 3262–3268, Jul. 2015.

[23] J. Li, M. W. Wen, X. Cheng, Y. Yan, S. Song, and M. H. Lee, "Differential spatial modulation with Gray coded antenna activation order," *IEEE Commun. Lett.*, vol. 20, no. 6, pp. 1100–1103, Jun. 2016.

[24] L. Yang, "Transmitter preprocessing aided spatial modulation for multiple-input multiple-output systems," in *Proc. IEEE 73rd Veh. Tech. Conf. (VTC Spring)*, May 2011, pp. 1–5.

[25] R. Zhang, L. Yang, and L. Hanzo, "Generalised pre-coding aided spatial modulation," *IEEE Trans. Wireless Commun.*, vol. 12, no. 11, pp. 5434–5443, Nov. 2013.

[26] A. StavridiM, M. Di Renzo, and H. Haas "Performance analysis of multi-stream receive spatial modulation in the MIMO broadcast channel," *IEEE Trans. Wireless Commun.*, vol. 15, no. 3, pp. 1808–1820, Mar. 2016.

[27] J. Li, M. Wen, X. Cheng, Y. Yan, S. Song, and M. H. Lee, "Generalised pre-coding aided quadrature spatial modulation," *IEEE Trans. Veh. Technol.*, 2016, to be published.

[28] A. Stavridis, D. Basnayak, S. Sinanovic, M. Di Renzo, and H. Haas, "A virtual MIMO dual-hop architecture based on hybrid spatial modulation," *IEEE Trans. Commun.*, vol. 62, no. 9, pp. 3161–3179, Sep. 2014.

[29] M. Zhang, M. Wen, X. Cheng, and L. Yang "A dual-hop virtual MIMO architecture based on hybrid differential spatial modulation," *IEEE Trans. Wireless Commun.*, vol. 15, no. 9, pp. 6356–6370, Sep. 2016.

[30] M. Di Renzo and H. Haas, "Bit error probability of SM-MIMO over generalized fading channels," *IEEE Trans. Veh. Technol.*, vol. 61, no. 3, pp. 1124–1144, Mar. 2012.

[31] M. D. Renzo and H. Haas, "On transmit diversity for spatial modulation mimo: Impact of spatial constellation diagram and shaping filters at the transmitter," *IEEE Trans. Veh. Technol.*, vol. 62, no. 6, pp. 2507–2531, Jul. 2013.

[32] M. Simon and M. S. Alaouni, *Digital Communications Over Fading Channels*. New York, NY, USA: Wiley, 2005.

[33] I. S. Gradshteyn and I. M. Rhyhik, *Table of Integrals, Series and Products*, 7th ed. New York, NY, USA: Academic, 2007.

[34] D. Samardzija and N. Mandayam, "Pilot-assisted estimation of MIMO fading channel response and achievable data rates," *IEEE Trans. Signal Process.*, vol. 51, no. 11, pp. 2882–2890, Nov. 2003.

[35] B. Hassibi and B. M. Hochwald, "How much training is needed in multiple-antenna wireless links?" *IEEE Trans. Inf. Theory*, vol. 49, no. 4, pp. 951–963, Apr. 2003.

[36] D. Zhang, G. Wei, J. Zhu, and Z. Tian, "On the bounds of feedback rates for pilot-assisted MIMO systems," *IEEE Trans. Veh. Technol.*, vol. 56, no. 4, pp. 1727–1736, Jul. 2007.

[37] W. M. Gifford, M. Z. Win, and M. Chiani, "Diversity with practical channel estimation," *IEEE Trans. Wireless Commun.*, vol. 4, no. 4, pp. 1935–1947, Jul. 2005.

[38] A. T. James, "Distributions of matrix variates and latent roots derived from normal samples," *Ann. Math. Statist.*, vol. 35, no. 2, pp. 475–501, 1964.

[39] M. Chiani and D. Dardari, "Improved exponential bounds and approximation for the Q-function with application to average error probability computation," in *Proc. IEEE Global Telecommun. Conf.*, Bologna, Italy, 2002, pp. 1399–1402.

[40] J. G. Proakis, *Digital Communications*, 3rd ed. New York, NY, USA: McGraw-Hill, 1995.

[41] Z. Wang and G. B. Giannakis, "A simple and general parameterization quantifying performance in fading channels," *IEEE Trans. Commun.*, vol. 51, no. 8, pp. 1389–1398, Aug. 2003.

JUN LI received the B.S. degree from South Central University for Nationalities, Wuhan, China, in 2009, and the M.S. degree from Chonbuk National University, Jeonju, South Korea, in 2011, where he is currently pursuing the Ph.D. degree. He had participated in the World Class University Project, sponsored by the National Research Foundation of Korea Grant funded by the Korean Ministry of Education Science and Technology as a Vice Head Researcher. His research interests include spatial modulation and OFDM schemes.

MIAOWEN WEN (M'14) received the B.S. degree from Beijing Jiaotong University, Beijing, China, in 2009, and the Ph.D. degree from Peking University, Beijing, in 2014. From 2012 to 2013, he was a Visiting Student Research Collaborator with Princeton University, Princeton, NJ, USA. Since 2014, he has been a Faculty Member at the South China University of Technology, Guangzhou, China. He has authored over 50 papers in refereed journals and conference proceedings. His recent research interests include spatial modulation and non-orthogonal multiple access techniques.

Dr. Wen was a recipient of the Best Paper Award from the IEEE International Conference on Intelligent Transportation Systems Telecommunications 2012, the IEEE International Conference on Intelligent Transportation Systems 2014, and the IEEE International Conference on Computing, Networking, and Communications 2016.

MENG ZHANG was born in Shandong, China. He received the B.S. degree in electronics engineering from the School of Electronics Engineering and Computer Science, Peking University, China, in 2014, where he is currently pursuing the M.S. degree in signal and information processing with the Modern Communications Research Institute. His research interests include spatial modulation, OFDM, and wireless powered communications. He was a recipient of the IEEE Microsoft Student Application Paper Grants.

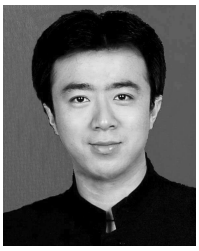

XIANG CHENG (S'05–M'10–SM'13) received the joint Ph.D. degree from Heriot-Watt University and the University of Edinburgh, Edinburgh, U.K., in 2009, where he received the Postgraduate Research Thesis Prize.

He has been an Assistant Professor with Peking University, Beijing, China, since 2010, and an Associate Professor since 2012. He has authored over 120 research papers in journals and conference proceedings. His research interests include mobile propagation channel modeling and simulation, next generation mobile cellular systems, intelligent transportation systems, and hardware prototype development.

Dr. Cheng was a recipient of the IEEE Leonard G. Abraham Prize (the IEEE JSAC best paper award) in 2016, and received several Best Paper Awards at the IEEE International Conference on ITS Telecommunications in 2012, the IEEE International Conference on Communications in China in 2013, the IEEE International Conference on Intelligent Transportation Systems in 2014, and the IEEE International Conference on Communications in 2016. He received the 2009 Chinese National Award for Outstanding Overseas Ph.D. Student and the 10th 2015 IEEE Asia Pacific Outstanding Young Researcher Award for his academic excellence and outstanding performance. He has served as the Symposium Leading Chair, the Co-Chair, and a member of the Technical Program Committee for several international conferences.